Article

Study on the Energy Efficiency Improvement and Operation Optimization of a Solar Water Heating System

Dawei Huang [1], Hongting Ma [1,2], Shuo Ma [2,*], Mo Chen [1], Chang Xu [1], Yongyichuan Zhang [1] and Cong Yan [1]

[1] Tianjin Key Laboratory of Indoor Air Environmental Quality Control, School of Environmental Science and Engineering, Tianjin University, Tianjin 300072, China; 2020214016@tju.edu.cn (D.H.); mht116@tju.edu.cn (H.M.); 1019214004@tju.edu.cn (M.C.); 1021214004@tju.edu.cn (C.X.); zhangyychuan@163.com (Y.Z.); yancong9721@163.com (C.Y.)

[2] Tianjin Key Laboratory of Built Environment and Energy Application, Tianjin University, Tianjin 300072, China

* Correspondence: ms0305@tju.edu.cn

Abstract: The solar-assisted electric boiler water heating systems adopted in student apartments at universities have some shortcomings, such as unsuitable system designs, unstable water supply temperature, and excessive power consumption. As discussed in this paper, the hot water supply system was reformed, and two apartments with the same building area, same solar collector area, and similar water consumption were selected to be used in comparative experiments. The auxiliary heat source for one of the apartments was changed from an electric boiler to three air source heat pumps, and a constant temperature water tank was added to form a double-tank water supply system. In addition, the operation strategy was adjusted. The other apartment was not modified. The energy consumption, solar fraction, water supply quality and economy of the two systems were analyzed and compared. The results showed that the transformation plan is reasonable and feasible. The solar fraction of the reformed system was significantly improved. The water supply temperature of the original system ranged from 35 °C to 60 °C, but it was shown to stabilize between 40 °C and 50 °C after the transformation. The average power saving rate of the reformed system reached 72.70%, and this economic benefit is highly significant. Additionally, the TRNSYS simulation software was used to model and optimize the control of the system.

Keywords: solar energy; water heating system; air source heat hump; electric boiler

1. Introduction

With the rapid development of the global economy, living standards have been improving. Simultaneously, energy consumption is increasing sharply. As the largest energy consumer in the world, China's energy consumption accounted for 23.2% of the global consumption in 2017, of which building energy consumption accounted for more than 30% of the total social energy consumption [1,2]. Within building energy consumption, HVAC systems and domestic hot water systems consumed nearly 60% of the total energy [3].

Solar energy is a type of clean renewable energy with abundant reserves, the development and utilization of which can effectively resolve energy shortages [4]. In recent years, various countries have been actively developing solar energy technology [5,6], and solar water heating systems are one of the most mature and widely used technologies. According to data from 2011, the total installed capacity of solar water heaters in operation in China accounted for 65.3% of the installed capacity worldwide, and it is clear that China currently dominates the global solar water heater market [7]; however, there are also some disadvantages in the application of solar energy, which is seriously affected by local climate conditions, changes in supply at night, etc. Therefore, for solar water heating systems, auxiliary heat sources are usually needed to maintain normal supplies of hot water in rainy weather and at night.

Traditional auxiliary heat sources include coal boilers, oil boilers, gas boilers, electric boilers, and so on. The heat pump is a new energy-related technology that has received considerable attention in recent years [8]. The heat pump is an energy-saving device that uses high-level energy to make heat flow from a low-level heat source to a high-level heat source. During this process, only a small amount of electricity is consumed. The integration of a heat pump unit into a system can be strategizes to increase the performance level of the system and enhance the use of solar energy [9]. There are two main types of solar-assisted heat pump (SAHP) systems: direct expansion solar-assisted heat pump (DX-SAHP) systems and indirect-style solar-assisted heat pump (i-SAHP) systems. i-SAHP systems can be further divided into parallel-type, serial-type, and dual-source-type systems [10,11]. The concept of combining solar energy with heat pumps was first proposed by Jordan and Therkeld [12]. A solar-assisted, wastewater source, heat pump, hot water system was built in TRNSYS, which enabled a more stable hot water temperature in winter with a significant decrease in the energy consumption [13]. Following this, scholars in various countries carried out a large number of theoretical and experimental studies on different system forms.

The DX-SAHP combines a solar collector and a heat pump evaporator into a unit, in which the refrigerant absorbs solar energy evaporation directly [14]. Chow et al. [15] developed a numerical model of the DX-SAHP system. Then, based on the Typical Meteorological Year weather data of Hong Kong, an annual average coefficient of performance (COP) of 6.46 was obtained for the system, which meant it was clearly superior to the traditional heat pump system. Kong et al. [16] developed a simulation model to predict the thermal performance of a DX-SAHP system, and the simulation results agreed well with the experimental data. Chaturvedi et al. [17] conducted a detailed, long-term thermal economic analysis of the energy-saving potential and economic feasibility of a DX-SAHP system. The results indicated that the life cycle cost of the system could be minimized by optimizing the collector area. Li et al. [18] recommended and analyzed a DX-SAHP water heater experimental setup, the average COP of which was measured under the spring climate in Shanghai and was found to be 5.25. Based on this experiment, some methods to improve the thermal performance of each component and the entire water heater system were proposed. The solar collector in the i-SAHP system is completely separated from the evaporator of the heat pump, and this type of heat pump is more stable. Worldwide, considerable research has also been conducted. Freeman et al. [19] performed a comprehensive simulation study of three i-SAHP systems in parallel, including series and dual-source systems. Cai et al. [20] presented a dynamic model for the solar water heating mode of i-SAHP systems, and the results of the numerical simulation corresponded well with the experimental data. The conclusion was that the COP increased from 2.35 to 2.57 as the solar irradiation increased from 0 W/m^2 to 800 W/m^2. Under the weather conditions in London, UK, Li et al. [21] conducted theoretical and experimental research on a newly designed i-SAHP system. Simultaneously, a model for a solar thermal loop was established and verified with experimental data. To meet the need for domestic hot water in a high-performance house, Chu et al. [22] designed an i-SAHP system and used the TRNSYS simulation software to model and optimize the control of the system.

Moreover, a series of comparative experiments on water heating systems was carried out. Feng et al. [23] established a mathematical model to compare the performance of a heat-pump-assisted solar water heater with that of an electric-heating-equipment-assisted solar water heater. The results showed that the efficiency of the water heater was higher when a heat pump was used as an auxiliary heat source. Huang et al. [24] carried out a long-term test on an integral solar heat pump water heater. The average energy consumption measured was much lower than that of the traditional solar water heater. Aye et al. [25] compared the electricity consumption, costs and greenhouse gas emissions of a traditional solar hot water system, a traditional air source heat pump hot water system, and a solar heat pump water heating system in Australia. Subsequently, Zhong et al. [26] made a similar comparative study based on the experimental system he designed in Kunming,

China. Li et al. [27] conducted a comparative study on the economics of four different water heating systems, including electric water heaters, town gas water heaters, SAHP systems and conventional SWH systems in Hong Kong, China. It was found that the solar-assisted air source heat pump (SA-ASHP) system saved more energy and had the least global warming impact out of several SAHP systems. Sterling et al. [11] designed an i-SAHP model using TRNSYS software and compared it to a conventional solar domestic hot water system and an electric domestic hot water system. The results showed that the electrical consumption and operating costs of the i-SAHP system were the lowest.

However, there are few comparative studies regarding different types of solar water heating systems under the climatic conditions of Tianjin, China. As discussed in this paper, a parallel SA-ASHP system was designed to supply domestic hot water for student apartments at a university in Tianjin, the original auxiliary heat source of which was an electric boiler. A comparative experiment was carried out on the two systems to compare their solar fraction, water supply quality, energy consumption and economy. The main objective of this paper was to propose a transformation plan for the water heating system of a university apartment to achieve a constant temperature water supply and save energy and to verify its feasibility and effectiveness through experiments. In addition, the findings can provide a reference for the design of a hot water system for a new apartment at the university.

The remaining sections are organized as follows: In Section 2, the principles of the two water heating systems before and after the retrofit are introduced, and then, the test schemes are proposed. In Section 3, the test results are discussed and analyzed. In Section 4, the simulation model of the SA-ASHP hot water system is established in TRNSYS software to optimize the operation strategy. Section 5 outlines the conclusion drawn.

2. System Specification

2.1. System Apparatus and Operation Strategies

There are 44 student apartments at the selected university. The schematic diagram of the original solar-assisted electric boiler water heating system is shown in Figure 1.
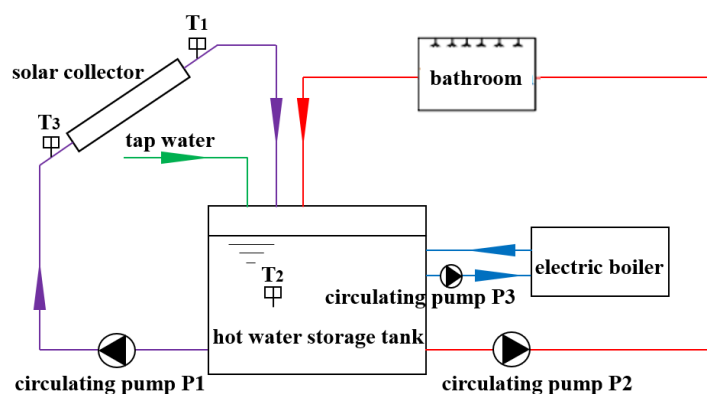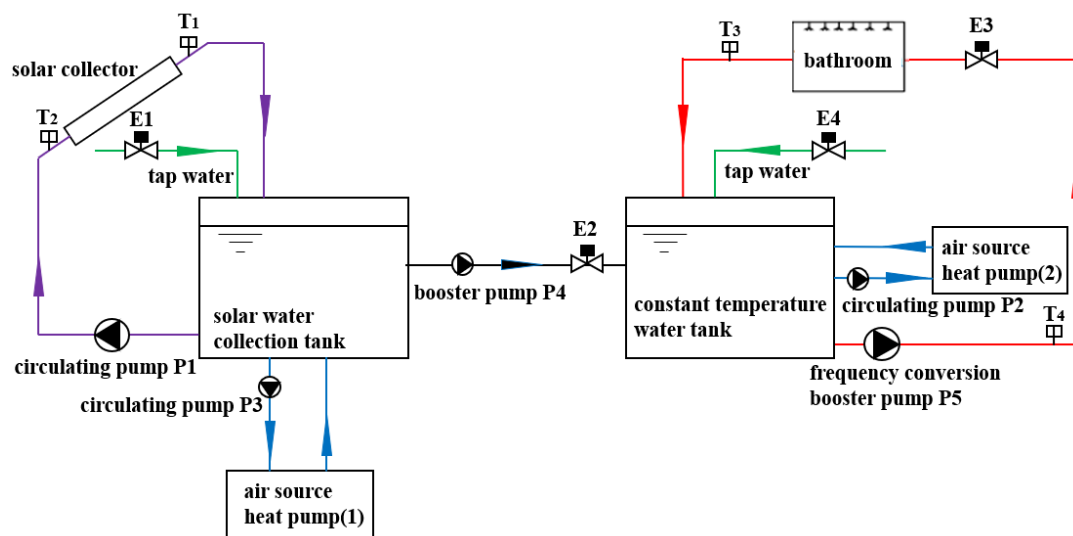

Figure 1. Schematic diagram of the original solar-assisted electric boiler water heating system.

It consists of a solar collector, an electric boiler, a hot water storage tank, etc. The collector installed on the roof has an area of 218 m². The hot water storage tank (volume 15 m³) and the electric boiler (120 kW) are mounted in the equipment room. The system's water supply temperature is 60 °C.

The operating strategies of the system are as follows: (i) Solar collector system: the collector temperature, T_1, rises with the increase in solar radiation intensity, and when $T_1 - T_2 \geq 7$ °C, the circulating pump, P1, opens. When $T_1 - T_2 \leq 3$ °C, the circulating pump, P1, stops. (ii) Water supply system: the water supply pump, P2, continuously operates for 24 h unless the water level in the tank is less than 0.1 m. (iii) Auxiliary heating system: like pump P2, the auxiliary heating water pump, P3, also operates for 24 h and will close when the water level in the tank is less than 0.1 m. During normal operation

of the system, the outlet temperature of pump P3 is monitored in real time, and when the temperature is <50 °C, all four of the heating tubes of the electric boiler are turned on. When the heating process occurs, the water temperature gradually increases, and when it increases to 53 °C, one heating tube is turned off. The second electric heating tube will be turned off when the temperature reaches 60 °C. When the outlet water temperature rises to 69 °C, all the heating tubes in the electric boiler will be turned off. (iv) Water supplement system: this system is controlled by the liquid level. The water supply valve is opened when the liquid level is lower than 1.5 m and closed when it reaches 1.8 m.

The two student apartments have the same building area and solar collector area and similar water consumption and usage modes. The hot water system of one of the student dormitories was reformed, while the other was not modified. The schematic diagram of the rebuilt SA-ASHP water heating system is shown in Figure 2.

Figure 2. Schematic diagram of the rebuilt SA-ASHP water heating system.

The transformation mainly consisted of:

(i). A new hot water storage tank (volume 6 m^3) was added as a solar water collection tank, and the original water tank with a volume of 15 m^3 was used as a constant temperature water tank. The two water tanks were connected to form a water supply system, and a thermostat was installed on the pipeline between them.

(ii). Three air source heat pumps were selected as auxiliary heat sources instead of the electric boiler. One was connected to the solar water collection tank, and the other two were set to control the temperature automatically and connected to the constant temperature water tank to form a constant temperature water supply system. The heat pump model was KFXRS-38II with a heating capacity of 38 kW.

(iii). To meet the student requirements for bath water temperature, to improve the efficiency of the air source heat pump and solar collector and to reduce the heat loss of solar collectors and hot water pipes, the water supply temperature was reduced from 60 °C to 40~50 °C.

The reformed system is equipped with a control system and a remote monitoring system, which can be monitored and measured remotely. In the control system, a programmable logic controller is used as the core control element, with the functions of timing, constant temperature, low water level water supply, over-temperature water replenishment and low-temperature water return. When the temperature of the water flowing from the solar water collection tank into the constant temperature water tank exceeds 50 °C, according to Figure 2, the solenoid valve E4 will be opened to replenish the cold water to the constant temperature water tank until the water temperature drops to 40 °C. The constant temperature water supply tank is connected with two air source heat pumps. When the

temperature of water flowing into the constant temperature water tank is lower than 40 °C, the heat pump will automatically begin to heat the water in the constant temperature water tank. When the water temperature reaches 50 °C, the two air source heat pumps turn off automatically. Therefore, the water supplied to the shower room is maintained within a reasonable range of 40~50 °C (the temperature setting can be adjusted according to seasonal variations). This control system also has protection alarm functions, such as for leakage, under-voltage and over-voltage. The water heating system operates automatically, and only one worker is required to monitor the parameters of the controller regularly.

2.2. Test Program

Both the original system and the reformed system can operate in different modes depending on the weather conditions. The difference between the original system and the reformed system is that the former system uses an electric boiler as an auxiliary heat source, while the latter uses an air source heat pump as an auxiliary heat source when the solar radiation does not meet the requirements. The physical diagrams of the main equipment in the solar and air source heat pump composite heat source domestic hot water supply system are shown in Figure 3.

| (a) | (b) | (c) |
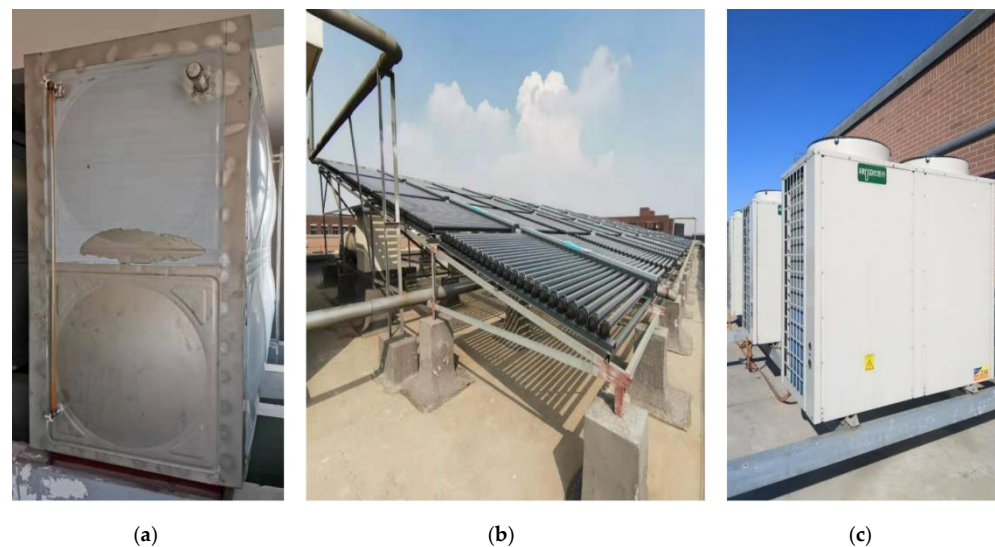
Figure 3. Main equipment of the system. (**a**) Water tank; (**b**) Solar collector; (**c**) Air source heat pump unit.

To carry out the comparative experiment, several measuring instruments were installed on the original system. Four ultrasonic heat meters were installed, respectively, on the water supply pipe, the return pipe, the water-replenishing pipe, and the collector circulation pipe to measure the temperature, the flow and the heat. An electric meter was installed to measure the power consumption of the electric boiler. A signal uploading system was created to collect and store real-time signals.

The testing of the two systems lasted for 135 days and was roughly divided into three stages: the heating period (2.18~3.14), transition season (3.15~6.14) and refrigeration period (6.15~7.2). The main test parameters included: solar energy collection, power consumption, hot water consumption and hot water supply temperature.

2.3. Uncertainty Analysis

Uncertainty is a parameter used to measure the quality of a result, indicating the range within which the estimated value is considered to be true [28]. Uncertainty is related to errors, which mainly include data processing errors, random errors and system device errors [29]. A data processing error usually derives from the calculation of the formula, which can be neglected. A random error can be avoided by repeated measurements.

Therefore, uncertainties in experiments only occur due to the measurement error of each instrument. The accuracies of the measuring instruments used in this experiment are shown in Table 1, and the error of the unit of hot water power consumption cannot be obtained directly but can be calculated using Equation (1):

$$\begin{cases} y = f(x_1, x_2, \ldots \ldots x_n) \\ U_y / y = \sqrt{\sum_{i=1}^{n} [(\partial f / \partial x_i) \times (U_{xi}/y)]^2} \end{cases} \tag{1}$$

where $x_1, x_2, \ldots \ldots x_n$ are direct measured parameters; y is an indirect calculated parameter; U_{xi} is the uncertainty of x_i.

Table 1. The accuracy of the measuring instruments.

Item	Water Temperature	Water Consumption	Heat Collection	Power Consumption
Instrument	Temperature sensor	Electromagnetic flowmeter	Electromagnetic heat meter	Electric energy meter
Model	PT100	SYA-D800-01X32	SYA-H200-01X65	DT862-4
Accuracy	±0.15%	±0.5%	±0.5%	±1%

The calculated error of the unit of hot water power consumption of the original solar-assisted electric boiler water heating system was 0.07%, and the error of the rebuilt system was also 0.07%. All the errors were controlled within 1%, indicating the reliability of the measured data.

3. Results and Discussion

Generally, climate conditions have an obvious effect on the performance of a solar water heating system and air source heat pump. Figure 4 shows the monthly average outdoor temperature, monthly sunshine h and monthly average daily radiation in Tianjin [30]. It is clear that the average outdoor temperature varies greatly in different seasons, which is much higher in summer than in winter. The highest average outdoor temperature is 26.4 °C in July. The monthly average daily radiation, in contrast, has little fluctuation throughout the year, varying from 14 MJ/(m^2·d) to 20 MJ/(m^2·d). The sunshine h do not change significantly. The peak value occurs in May, with a significant decline in June and a minimum in December.
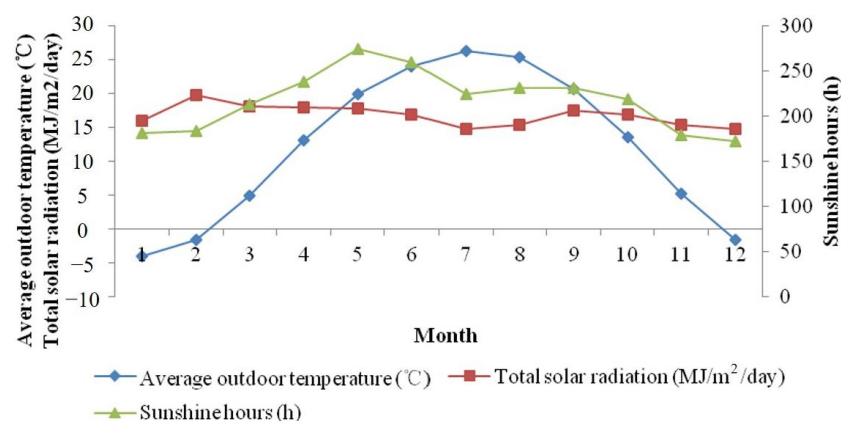
Figure 4. Climate conditions in Tianjin.

### 3.1. Comparison of Energy Consumption

To compare energy consumption before and after the water heating system reform, the daily power consumption and hot water consumption of the two systems during the period from 18 February to 2 July were measured. Both student apartments have

988 users. The energy consumption index comparisons between the two systems are summarized in Table 2. The results indicated that the SA-ASHP system has a high potential to save energy. After the transformation, the unit of hot water power consumption decreased from 37.40 kWh/m^3 to 10.51 kWh/m^3, and the per capita power consumption decreased from 1.10 kWh/day/person to 0.30 kWh/day/person. In addition, the daily water consumption per person declined significantly, because the water supply temperature was kept at 40~50 °C after the transformation, and the students could adjust the water temperature to appropriate levels more quickly when using hot water and could reduce unnecessary waste.

Table 2. Comparison of energy and water consumption indicators between the two solar water heating systems.

Item	Solar-Assisted Electric Boiler	SA-ASHP	Decline Rate
Unit of hot water power consumption (kWh/m^3)	37.40	10.51	71.90%
Per capita power consumption (kWh/day/person)	1.10	0.30	72.73%
Per capita water consumption (L/day/person)	31.05	27.79	10.50%

Figure 5 shows the average daily power consumption of the three stages. Both systems had the highest average daily power consumption during the heating period. This is because when the solar fraction is the smallest, the electric boiler and heat pumps need to be turned on for the longest time. After replacing the electric boiler with the air source heat pump as the auxiliary heat source, the average daily power consumption of the three periods decreased. The power consumption decreased from 1790 kWh to 485 kWh in the heating period, and the power saving rate reached 72.91%. During the entire test period, the average daily power saving was 790 kWh, and the average daily power saving rate was 72.70%. Based on these results, it can be estimated that the annual power saving of a hot water supply system in a student apartment would be about 288,350 kWh after the transformation.
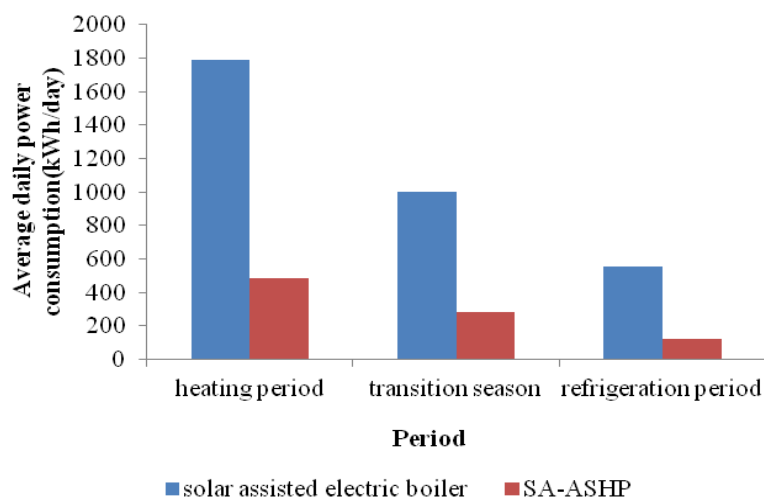
Figure 5. Average daily power consumption of the two water heating systems.

3.2. Variation in COP of the Air Source Heat Pump

The outdoor air temperature and the outlet water temperature have an obvious influence on the COP of air source heat pumps. In the present work, the effects of outdoor air temperature and the outlet water temperature on the COP of the air source heat pump were examined, and the results are shown in Figure 6.
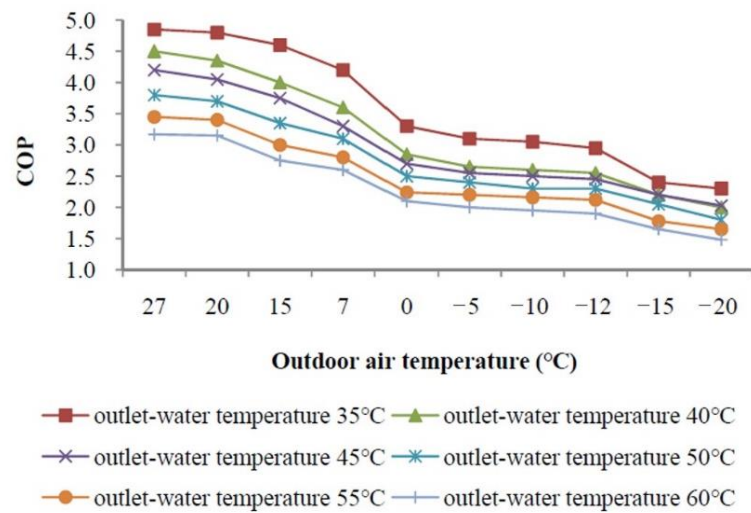
Figure 6. Performance curve of the air source heat pump.

According to Figure 6, at the same outlet water temperature, the COP of the heat pump unit gradually decreased with a decline in the outdoor air temperature, and the changing trend was basically identical for different water outlet temperatures. Figure 7 shows the monthly variations in the average outdoor temperature and the COP of the air source heat pump when the outlet water temperature was maintained at 45 °C. The average outdoor temperature in Tianjin was the lowest at −4 °C in January, and the COP of the heat pump unit was also the lowest of the year in January, with a value of 2.60. The outdoor temperatures in June, July and August were around 26 °C, making them the hottest three months of the year. During this period, the COP of the heat pump unit reached a peak as well, which was 4.20.
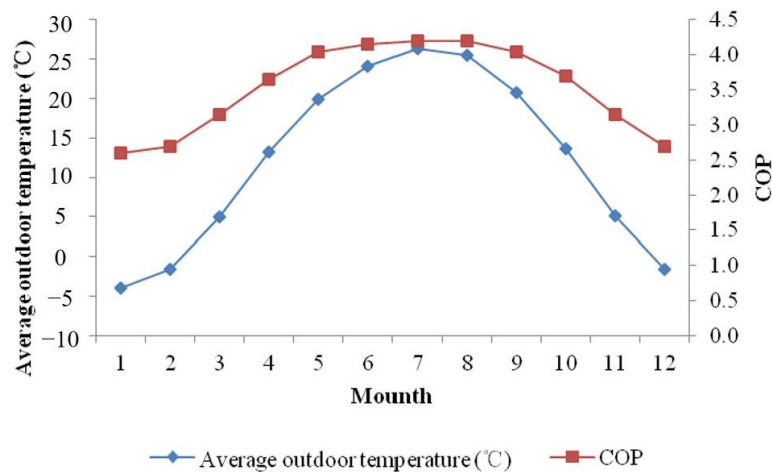

Figure 7. Variations in the average outdoor temperatures and the COP.

Based on Figure 7, taking the average temperature of 20 °C in May in Tianjin as an example, the curve of the COP of the air source heat pump in the system with the outlet water temperature could be obtained, as shown in Figure 8. It can be observed that when the outdoor air temperature was constant, the lower the outlet water temperature, the larger the COP. Therefore, reducing the set temperature of the water supply from 60 °C to 40~50 °C could effectively improve the COP of the water heating system by about 30%.
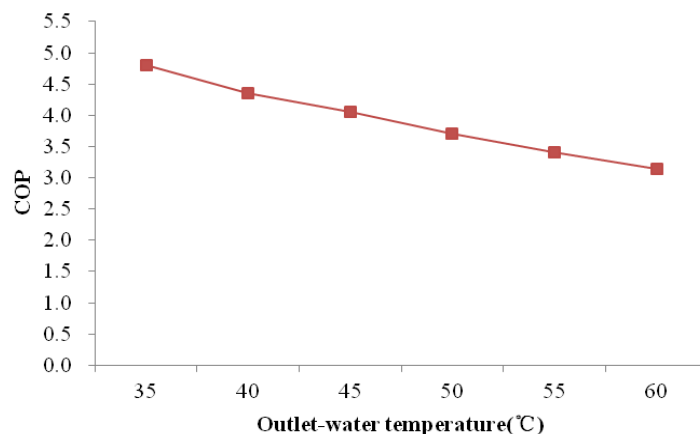
Figure 8. Variation in COP at an average temperature of 20 °C for different outlet water temperatures.

3.3. Solar Fraction Analysis

For a solar water heating system, the solar fraction, *f*, is one of the major evaluation indicators, reflecting the contribution rate of solar energy to the hot water system. It is defined as the percentage of the heat collection of a solar collector to the total heat of the system, which can be calculated as Equation (2):

$$f = Q_s/(Q_s + E_c) \times 100\% \tag{2}$$

where Q_s is the heat collected by the solar collector, MJ; E_c is the conventional energy consumption, MJ.

In the present work, heat collected by solar collectors in the two systems, the electric boiler power consumption and the electricity consumption of the air source heat pump were measured. Based on the data, the average solar fractions for the three stages of the heating period, the transition season and the refrigeration period were calculated. The final calculation results are shown in Table 3.

Table 3. Solar fraction of the two solar water heating systems.

| Item	Heating Period (2.18~3.14)	Transition Season (3.15~6.14)	Refrigeration Period (6.15~7.2)	Average Value
Solar-assisted electric boiler	14.4%	34.4%	70.2%	35.5%
SA-ASHP	49.9%	61.0%	90.6%	62.9%

As shown in Table 3, the solar fraction of the two systems varied greatly in different seasons and had the same variation tendency, meaning it was the highest in the refrigeration period and the lowest in the heating period. The reason for this is that the most sufficient solar energy was obtained in the refrigeration period, so the solar collector could function adequately; however, in the heating period, sunshine was inadequate; thus, the electric boiler or the heat pump was mainly relied upon to heat the water.

The results showed that the heat collected by the two solar collectors was similar in the same period, but the air source heat pumps consumed much less electricity than the electric boiler. By examining the comparisons of the solar fractions of the two systems, it can be noted that the value of the SA-ASHP system was much larger than that of the solar-assisted electric boiler water heating systems.
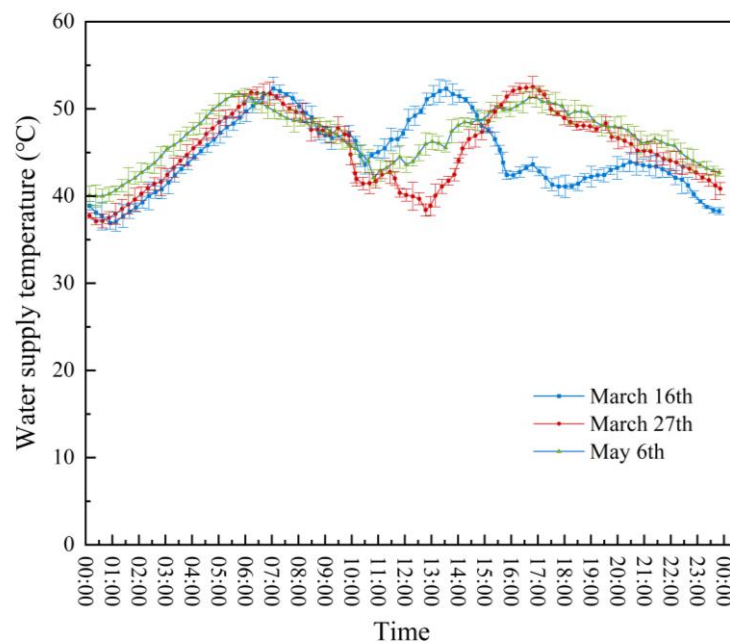
3.4. Water Supply Temperature Analysis

Three representative days were selected, which were 16 March, 27 March and 6 May, and the daily variations in the water supply temperature of the two hot water systems were recorded. The temperature was tested every 10 to 20 min. The results for the primary

solar-assisted electric boiler water heating system are shown in Figure 9, and the results of the rebuilt SA-ASHP water heating system are shown in Figure 10. In the measurement of water supply temperature, the average value of three equal-precision measurements plus the standard error was used for the analysis.
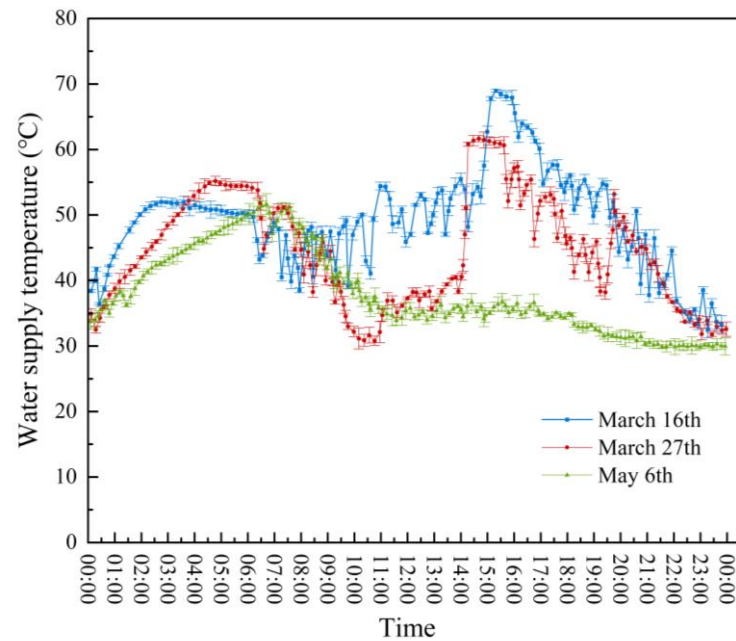
Figure 9. Water supply temperature of the solar-assisted electric boiler water heating system.

Figure 10. Water supply temperature of the SA-ASHP water heating system.

As can be observed in Figure 9, the actual hot water supply temperature of the original system fluctuated between 30 °C and 60 °C and occasionally reached 70 °C. There was a large fluctuation range, which was lower than the set value most of the time, so the quality of the hot water supply was not very good. In comparison, as shown in Figure 10, under the function of the constant temperature water tank, the water supply temperature of the reformed system could basically be stabilized between 40 °C and 50 °C, and the

quality of the water supply was noticeably improved, which could more effectively meet the demands of the students for hot water.

3.5. Economic Analysis

According to the data provided by the Logistics Support Department of the university, the price of electricity at this university is 0.505 Yuan/kWh. Thus, the annual electricity costs can be reduced by about 146 thousand Yuan after the reformation according to the results presented in Section 3.1. The payback period refers to the number of years required to recover the investment. The shorter the payback period, the more favorable the project. It is defined as Equation (3):

$$payback\ period = initial\ investment/cost\ saving\ per\ year \qquad (3)$$

The investment in energy efficiency improvement and the operation optimization of a solar water heating system included the design cost, technology development cost, equipment cost, material cost, transformation project cost, automatic control system development cost, operation commissioning cost, etc. The total investment for the reformation of each student apartment would be about 200 thousand Yuan, and the annual electricity saving would be about 146 thousand Yuan. Thus, the static investment recovery period would be about 16 months. The lifetime of the air source heat pump unit used in this system is 15 years.

4. TRNSYS Simulation and Operation Strategy Optimization

4.1. System Model and Results Comparison

According to the actual equipment parameters and system form of the SA-ASHP water heating system, a simulation model was established using TRNSYS software, and the simulation calculation results were compared with experimental test results to verify the accuracy of the simulation model. The TMY2 typical meteorological year generated using METEONORM software was used as a meteorological file for the simulation model. The subject had a latitude of 39°06′ N, a longitude of 117°10′ E, an altitude of 3.3 m, and the time zone is located in the East Eighth District.

This simulation model shown in Figure 11 included 12 types of simulation modules: a vacuum tube solar collector (Type 71), air source heat pump (Type 505b), water tank (Type 4c), water pump (Type 3b), meteorological data reading and processing (Type109-TMY2), temperature controller (Type 2b), water load distribution (Type 14h), supplemental water temperature distribution (Type 14e), integrator (Type 24), plotter (Type 65d), printer (Type 25c) and calculator. The water load distribution module and the make-up water temperature distribution module used the measured water consumption and tap water make-up temperature during the experimental test when the distribution function was written, thereby improving the accuracy of the simulation model and reducing the error from the theoretically assumed water load and make-up temperature zone.

The relative errors between the simulated results and the measured results of solar heat collection, air source heat pump heating and solar energy contribution rates were 2.90%, 4.66% and 3.83%, respectively. The relative error of each parameter was small, which indicated that the simulation results were in good agreement with the measured results, which verified the accuracy of the established simulation model.

4.2. Operation Strategy Optimization

As mentioned in Section 2.1, the start temperature difference in the heat collection cycle of the SA-ASHP water heating system was set to 7 °C, and the stop temperature difference was set to 3 °C. When the solar radiation intensity was strong, by optimizing the heat collection cycle operation control strategy and appropriately reducing the starting temperature difference and stopping temperature difference, it could effectively increase the running time of the heat collection cycle, thereby improving the solar energy guarantee rate of the system. The researchers changed the temperature difference, ΔT_H, and the lower

limit of temperature difference, ΔT_L, of the thermal cycle temperature difference controller in the simulation model to 6 °C and 2 °C; 5 °C and 1 °C, respectively, and called them optimization scheme 1 and optimization scheme 2, respectively. Through the simulation calculation of the two optimization schemes, a comparison table of the annual operating data of the main parameters of the system after the optimization of the heat collection cycle operation control strategy was obtained.
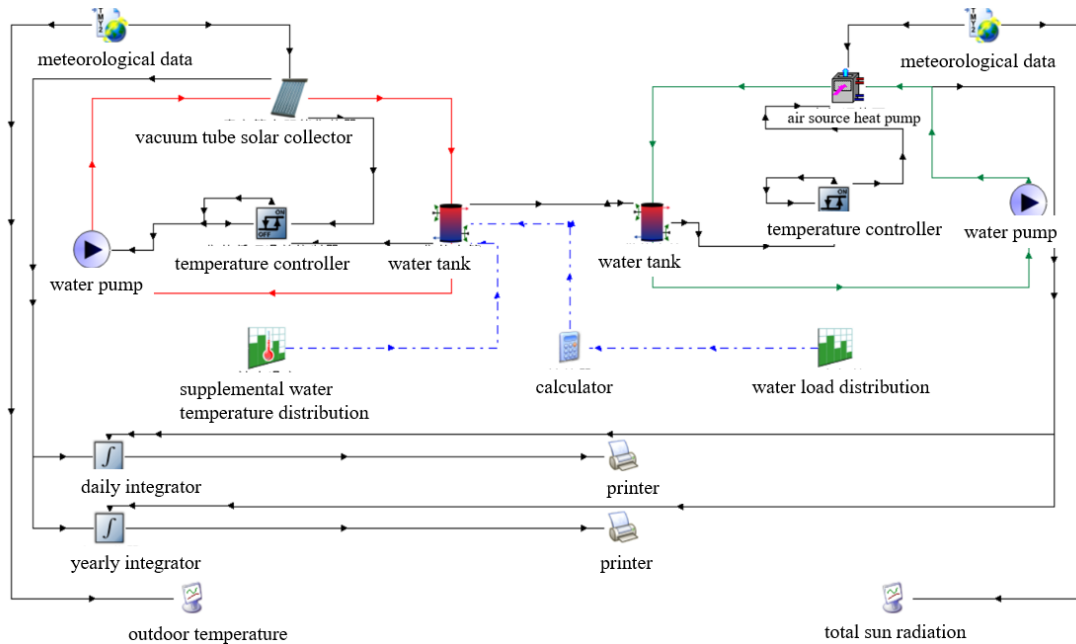
Figure 11. The simulation model of SA-ASHP water heating system in TRNSYS.

It can be determined from Table 4 that by optimizing the heat collection cycle operation control strategy, the solar heat collection and solar energy guarantee rate are both improved and the air source heat pump heating capacity is reduced. Through optimization scheme 1, the system's annual solar heat collection increased from 334,121.56 MJ to 367,166.55 MJ, an increase of 9.89%, and the system's solar guarantee rate increased from 32.76% to 38.10%, an increase of 16.30%. Through optimization scheme 2, the system's annual solar heat collection increased from 334,121.56 MJ to 388,513.44 MJ, an increase of 16.28%, and the system's solar guarantee rate increased from 32.76% to 41.26%, an increase of 25.95%.

Table 4. Comparison of main parameters after optimization of operation control strategy.

Scheme	ΔT_H (°C)	ΔT_L (°C)	Heat Collected by the Solar Collector (MJ)	Heat Collected by the Air Source Heat Pump (MJ)	Solar Assurance Rate (Calculated Based on Total Annual Heat Value) (%)
Original scheme	7	3	334,121.56	685,920.63	32.76
Optimization scheme 1	6	2	367,166.55	596,452.72	38.10
Optimization scheme 2	5	1	388,513.44	553,161.79	41.26

5. Conclusions

As discussed in this paper, due to some of the drawbacks of the solar-assisted electric boiler water heating system of a university student apartment in Tianjin, a new SA-ASHP water heating system was designed. Comparative experiments were carried out using these two systems. The main conclusions are as follows:

(i). The COP of the air source heat pump increases with increasing outdoor air temperature and a decrease in outlet water temperature. The COP of the water-heating system can be effectively improved by changing the set value of the water supply temperature from 60 °C to 40~50 °C, which is about 30% higher.

(ii).　The solar fraction has obvious differences in different seasons, with the highest in the refrigeration period and the lowest in the heating period. Compared with the original solar-assisted electric boiler water heating system, the solar fraction of the SA-ASHP system is much larger.

(iii).　The comparison results of the water supply temperatures for the three days selected indicated that the reformed SA-ASHP water heating system has a greater water supply quality, and the temperature can be approximately stabilized between 40 °C and 50 °C.

(iv).　After using the air source heat pump as an auxiliary heat source, the energy consumption indexes, such as the unit of hot water power consumption, per capita power consumption, and per capita water consumption, decreased significantly, the energy saving rate reached 72.70%, and the economic benefits of the system were greatly improved.

(v).　By optimizing the heat collection cycle operation control strategy, the solar heat collection and solar energy guarantee rate are both improved, and the air source heat pump heating capacity is reduced.

Institutional Review Board Statement: Not applicable.

Informed Consent Statement: Not applicable.

Data Availability Statement: Not applicable.

Conflicts of Interest: The authors declare that they have no conflict of interest in this work, and declare that they do not have any commercial or associative interest that represents a conflict of interest in connection with the work submitted.

References

1.　Petroleum, B. Bp statistical review of world energy 2018. *Sustainability* **2018**, *10*, 17.

2.　Zhan, J.; Liu, W.; Wu, F.; Li, Z.; Wang, C. Life cycle energy consumption and greenhouse gas emissions of urban residential buildings in Guangzhou city. *J. Clean. Prod.* **2018**, *194*, 318–326. [CrossRef]

3.　Ma, H.T.; Yu, S.J.; Li, C.; Zhang, Z.Y.; Gao, F.; Du, N. Influence of rubber ball on-line cleaning device on chiller performance. *Appl. Therm. Eng.* **2018**, *128*, 1488–1493. [CrossRef]

4.　Frattolillo, A.; Canale, L.; Ficco, G.; Mastino, C.C.; Dell'Isola, M. Potential for building façade-integrated solar thermal collectors in a highly urbanized context. *Energies* **2020**, *13*, 5801. [CrossRef]

5.　Winston, D.P.; Pounraj, P.; Manokar, A.M.; Sathyamurthy, R.; Kabeel, A. Experimental investigation on hybrid PV/T active solar still with effective heating and cover cooling method. *Desalination* **2018**, *435*, 140–151.

6.　Pounraj, P.; Winston, D.P.; Kabeel, A.; Kumar, B.P.; Manokar, A.M.; Sathyamurthy, R.; Christabel, S.C. Experimental investigation on peltier based hybrid PV/T active solar still for enhancing the overall performance. *Energy Convers. Manag.* **2018**, *168*, 371–381. [CrossRef]

7.　Qiu, S.F.; Ruth, M.; Ghosh, S. Evacuated tube collectors: A notable driver behind the solar water heater industry in China. *Renew. Sustain. Energy Rev.* **2015**, *47*, 580–588. [CrossRef]

8.　Jung, Y.; Oh, J.; Han, U.; Lee, H. A comprehensive review of thermal potential and heat utilization for water source heat pump systems. *Energy Build.* **2022**, *266*, 112124. [CrossRef]

9.　Pinamonti, M.; Beausoleil-Morrison, I.; Prada, A.; Baggio, P. Water-to-water heat pump integration in a solar seasonal storage system for space heating and domestic hot water production of a single-family house in a cold climate. *Sol. Energy* **2021**, *213*, 300–311. [CrossRef]

10.　Kim, T.; Choi, B.I.; Han, Y.S.; Do, K.H. A comparative investigation of solar-assisted heat pumps with solar thermal collectors for a hot water supply system. *Energy Convers. Manag.* **2018**, *172*, 472–484. [CrossRef]

11.　Sterling, S.J.; Collins, M.R. Feasibility analysis of an indirect heat pump assisted solar domestic hot water system. *Appl. Energy* **2012**, *93*, 11–17. [CrossRef]

12.　Jordan, R.; Threlkeld, J. Design and economics of solar energy heat pump system. *Heat. Pip. Air Cond.* **1954**, *26*. Available online: https://www.osti.gov/biblio/7096314 (accessed on 14 July 2022).

13. Zhang, D.; Gao, Z.; Fang, C.; Shen, C.; Li, H.; Qin, X. Simulation and analysis of hot water system with comprehensive utilization of solar energy and wastewater heat. *Energy* **2022**, *253*, 124181. [CrossRef]

14. Kuang, Y.; Sumathy, K.; Wang, R. Study on a direct-expansion solar-assisted heat pump water heating system. *Int. J. Energy Res.* **2003**, *27*, 531–548. [CrossRef]

15. Chow, T.T.; Pei, G.; Fong, K.F.; Lin, Z.; Chan, A.L.S.; He, M. Modeling and application of direct-expansion solar-assisted heat pump for water heating in subtropical Hong Kong. *Appl. Energy* **2010**, *87*, 643–649. [CrossRef]

16. Kong, X.; Zhang, D.; Li, Y.; Yang, Q. Thermal performance analysis of a direct-expansion solar-assisted heat pump water heater. *Energy* **2011**, *36*, 6830–6838. [CrossRef]

17. Chaturvedi, S.K.; Gagrani, V.D.; Abdel-Salam, T.M. Solar-assisted heat pump—A sustainable system for low-temperature water heating applications. *Energy Convers. Manag.* **2014**, *77*, 550–557. [CrossRef]

18. Li, Y.; Wang, R.; Wu, J.; Xu, Y. Experimental performance analysis on a direct-expansion solar-assisted heat pump water heater. *Appl. Therm. Eng.* **2007**, *27*, 2858–2868. [CrossRef]

19. Freeman, T.; Mitchell, J.; Audit, T. Performance of combined solar-heat pump systems. *Sol. Energy* **1979**, *22*, 125–135. [CrossRef]

20. Cai, J.Y.; Ji, J.; Wang, Y.Y.; Huang, W.Z. Numerical simulation and experimental validation of indirect expansion solar-assisted multi-functional heat pump. *Renew. Energy* **2016**, *93*, 280–290. [CrossRef]

21. Li, L.; Ge, Y.T.; Zavareh, M.T. Performance evaluation of an indirect solar assisted heat pump system for domestic hot water production. In *Refrigeration Science and Technology, Proceedings of the 3rd IIR International Conference on Sustainability and the Cold Chain, London, UK, 23–25 June 2014*; International Institute of Refrigeration: Paris, France, 2014.

22. Chu, J.; Choi, W.; Cruickshank, C.A.; Harrison, S.J. Modeling of an indirect solar assisted heat pump system for a high performance residential house. *J. Sol. Energy Eng. Trans. ASME* **2014**, *136*, 041003. [CrossRef]

23. Shiyu, F.; Wei, H.; Xiufeng, G. Annual operating property of heat pump assisted solar central water heater. *Acta Energ. Sol. Sin.* **2008**, *29*, 283.

24. Huang, B.J.; Lee, C.P. Long-term performance of solar-assisted heat pump water heater. *Renew. Energy* **2004**, *29*, 633–639. [CrossRef]

25. Aye, L.; Charters, W.; Chaichana, C. Solar heat pump systems for domestic hot water. *Sol. Energy* **2002**, *73*, 169–175. [CrossRef]

26. Zhong, H.; Li, Z.-M.; Luo, H.-L.; Tie, Y.; Li, M.; Xia, C.-F. Experimental investigation of a solar water heater in conjunction with air source heat pump. *Constr. Conserves Energy* **2011**, *39*, 36–39.

27. Li, H.; Yang, H.X. Potential application of solar thermal systems for hot water production in Hong Kong. *Appl. Energy* **2009**, *86*, 175–180. [CrossRef]

28. Liang, R.B.; Pan, Q.G.; Wang, P.; Zhang, J.L. Experiment research of solar PV/T cogeneration system on the building facade driven by a refrigerant pump. *Energy* **2018**, *161*, 744–752. [CrossRef]

29. Ma, H.T.; Zhang, J.Y.; Liu, C.F.; Lin, X.Y.; Sun, Y.X. Experimental investigation on an adsorption desalination system with heat and mass recovery between adsorber and desorber beds. *Desalination* **2018**, *446*, 42–50. [CrossRef]

30. Ruicheng, Z. *Technical Guidebook for Solar Water Heating System of Civil Buildings*; Chemical Industry Press: Beijing, China, 2006.